

Identification of 3,4-Dihydroisoquinoline-2(1*H*)-sulfonamides as Potent Carbonic Anhydrase Inhibitors: Synthesis, Biological Evaluation, and Enzyme–Ligand X-ray Studies[†]

Rosaria Gitto,^{*,‡} Stefano Agnello,[‡] Stefania Ferro,[‡] Laura De Luca,[‡] Daniela Vullo,[§] Jiri Brynda,^{||,⊥} Pavel Mader,^{||,⊥} Claudiu T. Supuran,[§] and Alba Chimirri[‡]

[‡]*Dipartimento Farmaco-Chimico, Università di Messina, Viale Annunziata, I-98168 Messina, Italy*, [§]*Laboratorio di Chimica Bioinorganica, Università degli Studi di Firenze, Firenze, Italy*, ^{||}*Department of Structural Biology, Institute of Molecular Genetics, Academy of Sciences of the Czech Republic, CZ-16637 Prague, Czech Republic*, and [⊥]*Department of Structural Biology, Institute of Organic Chemistry and Biochemistry, Academy of Sciences of the Czech Republic, CZ-16637 Prague, Czech Republic*

Received September 21, 2009

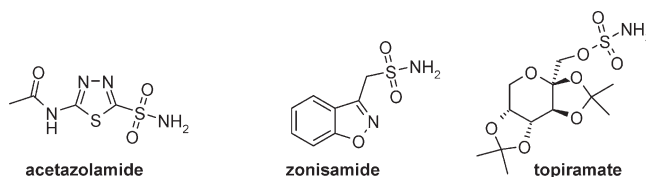
Following previous studies we herein report the exploration of the carbonic anhydrase (CA, EC 4.2.1.1) inhibitory effects and enzyme selectivity of a small class of 1-(cyclo)alkylisoquinolines containing a sulfonamide function considered a key feature for inhibiting CA. The results of enzymatic assays against human (h) CA isoforms, hCA I and hCA II (cytosolic, ubiquitous enzymes), hCA IX (transmembrane, tumor-associated), and hCA XIV (transmembrane), suggested that the presence of C-1 small substituents on isoquinoline scaffold controls both inhibitory potency and selectivity. Some derivatives showed potent hCA IX and hCA XIV inhibitory effects at nanomolar concentrations as well as low affinity for the ubiquitous hCA II. Moreover, we report the X-ray crystal structure of one of these derivatives in complex with dominant human isoform II, thus confirming the sulfonamide–zinc interactions. Finally, the results of docking experiments suggested the hypothetical interactions in the catalytic binding site for the most active and selective hCA IX and hCA XIV inhibitor.

Introduction

The carbonic anhydrases (CAs, EC 4.2.1.1) are a family of monomeric zinc metalloenzymes that catalyze the reversible hydration of CO₂. Since this reaction regulates a broad range of physiological functions, the pharmacological modulation of CA activity could be useful for the treatment of several human diseases. There are 15 human known CA (hCA^a) isoforms with different tissue distribution, expression levels, and subcellular locations. Some of these isozymes (e.g., hCA II, IV, VA, VB, VII, IX, XII, XIII, and XIV) constitute valid targets for the development of anticancer, antiglaucoma, antiobesity, or anticonvulsant drugs.^{1–8} However, the CA diffuse localization in many tissues and organs limits potential clinical applications. So the development of CA inhibitors (CAIs) possessing high potency and selectivity against some specific isoforms represents an attractive strategy to obtain pharmacological tools, thus avoiding side effects and improving therapeutic safety.

In particular, there is significant interest in the development of selective inhibitors targeting isozymes CAIX and CAXIV. In particular, CA IX is a peculiar member of the CA family, since it is expressed in a limited number of normal tissues (mainly the gastrointestinal tract), whereas its overexpression

Chart 1. Chemical Structures of the Carbonic Anhydrase Inhibitors: Acetazolamide, Zonisamide, and Topiramate



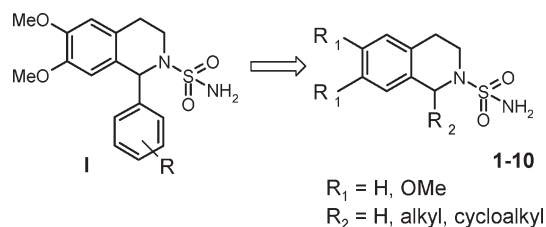
is seen on the cell surface of a large number of solid tumors showing inadequate supply of oxygen as key feature.⁵ This tumor hypoxia regulates the expression of several genes, including CA IX, through the hypoxia inducible factor 1 (HIF-1) cascade. Furthermore, CA IX overexpression is often associated with a poor responsiveness to the classical radiotherapy and chemotherapy. So the development of selective CAIX isoform inhibitors represents a new strategy to design anticancer drugs with a novel mechanism of action.⁹ Similar to CA IX, CA XIV is a transmembrane isozyme with the active site oriented extracellularly; it is highly abundant in neurons and axons in the murine and human brain, where it seems to play an important role in modulating excitatory synaptic transmission.¹⁰

Most of known CAIs contain a sulfonamide/sulfamate moiety able to coordinate the zinc ion of catalytic binding site (e.g., acetazolamide, zonisamide, and topiramate, Chart 1), inhibiting in this way the enzymatic activity.^{11–18} These inhibitors bear specific functional groups that interact with important amino acid residues, thus driving the selectivity against the different isoforms as confirmed by X-ray

[†]The atomic coordinates and crystal structure have been deposited in the Protein Data Bank as entry 3IGP.

^{*}To whom correspondence should be addressed. Phone: 00390906766413. Fax: 00390906766402. E-mail: rgitto@pharma.unime.it.

^aAbbreviations: hCA, human carbonic anhydrase; HIF-1, hypoxia inducible factor 1; MW, microwave; PDB, Protein Data Bank; rmsd, root-mean-square deviation; TFA, trifluoroacetic acid.

Chart 2. New Designed Isoquinoline Derivatives **1–10** as Carbonic Anhydrase Inhibitors

crystallographic data of complexes between CAIs and isozymes available in the literature.^{19–26}

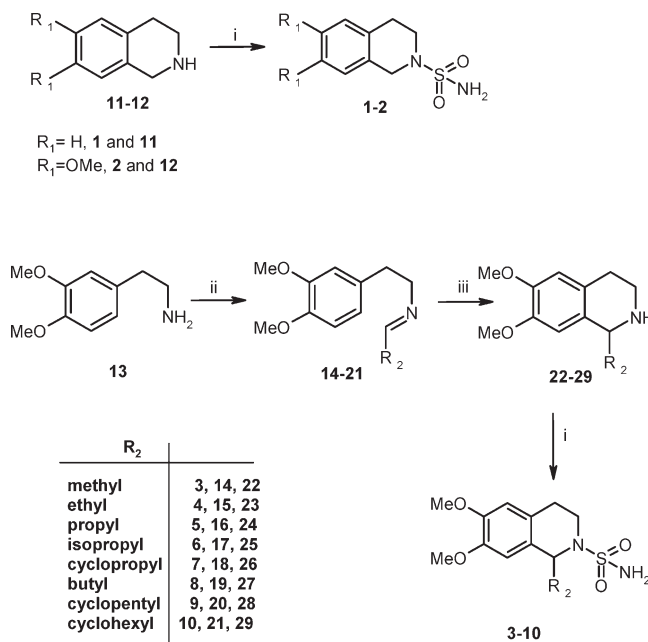
In a previous paper²⁷ we identified some 1-aryl-6,7-dimethoxy-3,4-dihydroisoquinoline-2(1*H*)-sulfonamides (**1**, Chart 2) that proved to inhibit some CA isoforms at micromolar concentration but show poor selectivity; our hypothesis was that the presence of bulky C-1 aryl substituent could produce steric hindrance for interaction between the sulfonamide group and the metal ion in the catalytic site.

So in this paper we extended our study to a new series of 3,4-dihydroisoquinoline-2(1*H*)-sulfonamides (**1–10**, Chart 2) containing some structural modifications in search of the enhancement of both activity and selectivity. In particular, (a) to evaluate the steric and electronic effects, we planned the replacement of the C-1 aryl substituent with alkyl and cycloalkyl groups; (b) to test the role of the substituents on the isoquinoline scaffold, we synthesized compounds lacking of the C-1 substituent as well as the two methoxy groups. The synthesis of target compounds was accomplished in microwave conditions and the screening against some relevant CA isoforms was performed. In particular, the obtained compounds were tested against the two physiologically human cytosolic hCA I and hCA II isozymes, the tumor-associated transmembrane isoform hCA IX, and the neuronal hCA XIV isoform.

Moreover, we report the X-ray crystal structure of the dominant hCA II isoform complexed with a new derivative, allowing the determination of the sulfonamide–zinc interactions in the catalytic binding site. Docking experiments have been performed with the aim to identify the interactions promoting the selectivity toward hCA IX and hCA XIV isoforms.

Results and Discussion

Chemistry. The synthetic pathways for the 3,4-dihydroisoquinoline-2(1*H*)-sulfonamides (**1–10**) can be found in Scheme 1. Derivatives **1** and **2** were readily synthesized in microwave conditions starting from commercially available isoquinolines **11** and **12** and a large excess of sulfamide as previous reported by us.²⁷ The precursors 1-(cyclo)alkyl-6,7-dimethoxy-1,2,3,4-tetrahydroisoquinoline **22–29** were prepared in accordance with an optimized microwave-assisted approach through the Pictet–Spengler condensation.^{27,28} Starting from the commercially available 2-(3',4'-dimethoxyphenyl)ethylamine (**13**), the imine intermediates **14–21** were obtained by reaction with the appropriate aldehyde in solvent-free conditions and successively cyclized in acidic medium to give the desired compounds **22–29**. Finally, the intermediates **22–29** were coupled with a large excess of sulfamide, affording the corresponding 6,7-dimethoxy-3,4-dihydroisoquinoline-2(1*H*)-sulfonamides (**3–10**). The structures of all obtained compounds were supported by elemental analyses and spectroscopic measurements.

Scheme 1. Synthesis of 3,4-Dihydroisoquinoline-2(1*H*)-sulfonamides (**1–10**)^a

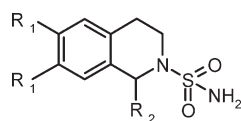
^a Reagents and conditions. (i) $\text{CH}_3\text{CH}(\text{OCH}_3)_2$, $\text{NH}_2\text{SO}_2\text{NH}_2$, two steps in the same conditions: 20 min, 100 °C, 200 psi, 150 W. (ii) R_2CHO , MW: 5 min, 90 °C, 200 psi, 150 W. (iii) TFA, MW: 5 min, 90 °C, 200 psi, 150 W.

Carbonic Anhydrase Inhibition. To determine the enzymatic inhibitory activity, the new series of 6,7-dimethoxy-3,4-dihydroisoquinoline-2(1*H*)-sulfonamides (**1–10**) was assayed on four important carbonic anhydrase isoforms involved in several physiological and pathological processes, hCA I, hCA II, hCA IX, and hCA XIV (Table 1).

The enzymatic screening showed that the 3,4-dihydroisoquinoline-2(1*H*)-sulfonamides **1–10** have a moderate inhibitory activity against human carbonic anhydrase I (hCA I), with inhibition constants (K_i) in the range 0.10–6.41 μM (see Table 1).

Our biological data reported in Table 1 highlighted that the isozyme hCA II was inhibited by the 6,7-dimethoxy-3,4-dihydroisoquinoline-2(1*H*)-sulfonamides (**1–10**) with K_i values ranking from 32.8 nM to 350 μM , suggesting that there is significant impact of the size of the C-1 substituent on inhibitory efficacy; in fact the most active sulfonamide derivatives of this series were unsubstituted and methyl-substituted derivatives **1**, **2**, and **3**. For the other (cyclo)alkyl derivatives **4–10** the inhibitory effects were much lower than those of compounds **1–3**. In particular, the 6,7-dimethoxy-1-propyl-3,4-dihydroisoquinoline-2(1*H*)-sulfonamide (**5**) and the corresponding superior homologous 6,7-dimethoxy-1-butyl-3,4-dihydroisoquinoline-2(1*H*)-sulfonamide (**8**) were about 2500- to 3700-fold less active than the parent unsubstituted 6,7-dimethoxy-3,4-dihydroisoquinoline-2(1*H*)-sulfonamide (**2**) on hCA II; it is probably due to the key role of C-1 substituent in the recognition process into the active catalytic site.

All synthesized compounds **1–10** demonstrated generally very high and similar potency against hCA IX and hCA XIV isoforms with a significant variation of the inhibitory effects that appear related to the nature of C-1 substituent. We found that the unsubstituted ($R_2 = \text{H}$) derivatives **1** and **2** as well as derivatives containing small (cyclo)alkyl substituents

Table 1. Inhibition of hCA I, hCA II, hCA IX, and hCA XIV Isoforms by 6,7-Dimethoxy-3,4-dihydroisoquinoline-2(1*H*)-sulfonamides (**1–10**), 6,7-Dimethoxy-1-phenyl-3,4-dihydroisoquinoline-2(1*H*)-sulfonamide (**I**), Zonisamide, Acetazolamide, and Topiramate and Selectivity Ratios $K_I(\text{hCAII})/K_I(\text{hCAIX})$ and $K_I(\text{hCAII})/K_I(\text{hCAXIV})$ 

| R ₁ | R ₂ | compd | K_I (nM) ^a | | | | selectivity ratios ^b | |
|----------------------------|------------------|-----------------------|-------------------------|--------|--------|---------|---------------------------------------|--|
| | | | hCA I | hCA II | hCA IX | hCA XIV | $K_I(\text{hCAII})/K_I(\text{hCAIX})$ | $K_I(\text{hCAII})/K_I(\text{hCAXIV})$ |
| H | H | 1 | 1510 | 32.8 | 3.7 | 6.0 | 8.86 | 5.47 |
| MeO | H | 2 | 6410 | 94.5 | 9.5 | 9.8 | 9.95 | 9.64 |
| MeO | methyl | 3 | 2800 | 87.3 | 9.4 | 9.6 | 9.29 | 9.09 |
| MeO | ethyl | 4 | 1820 | 1975 | 76.3 | 2754 | 25.9 | 0.72 |
| MeO | <i>n</i> -propyl | 5 | 3150 | 235000 | 330 | 302 | 712.12 | 778.15 |
| MeO | isopropyl | 6 | 3780 | 1050 | 6.1 | 4.7 | 172.13 | 223.40 |
| MeO | cyclopropyl | 7 | 3950 | 820 | 8.5 | 6.4 | 96.47 | 128.13 |
| MeO | <i>n</i> -butyl | 8 | 4100 | 350000 | 400 | 1650 | 875.00 | 212.12 |
| MeO | cyclopentyl | 9 | 100 | 650 | 55 | 178 | 11.82 | 3.65 |
| MeO | cyclohexyl | 10 | 1180 | 18890 | 706 | 7950 | 26.76 | 2.38 |
| MeO | phenyl | I ^c | 8980 | 15700 | 8440 | 3860 | 1.86 | 4.07 |
| acetazolamide ^d | | | 250 | 12 | 25 | 41 | 0.48 | 0.29 |
| zonisamide ^d | | | 56 | 35 | 5.1 | 5250 | 6.86 | <0.01 |
| topiramate ^d | | | 250 | 10 | 58 | 1460 | 0.17 | <0.01 |

^a Errors in the range of $\pm 10\%$ of the reported value, from three different assays. Recombinant full length hCA I, II, and XIV and catalytic domain of hCA IX were used. ^b The K_I ratios indicate the inhibition selectivity. ^c From ref 27. ^d From ref 5.

(e.g., **3**, **6**, and **7**) showed the strongest inhibitory activity at nanomolar concentration against hCA IX and hCA XIV isoforms with inhibition constants in the range 3.7–9.5 nM for hCA IX and 4.7–9.8 nM for hCA XIV. The best inhibitor was the 6,7-dimethoxy-1-isopropyl-3,4-dihydroisoquinoline-2(1*H*)-sulfonamide (**6**) showing K_I values of 6.1 and 4.7 nM against hCA IX and hCA XIV, respectively. Furthermore compound **4** (R_2 = ethyl) showed significant selectivity for inhibiting hCA IX (K_I of 76.3 nM) over hCA XIV (K_I of 2754 nM). We observed that the presence of bulky (cyclo)alkyl groups (e.g., **5**, **8**, **9**, and **10**) led to a decrease of the activity, with K_I in the range 55.0–706 nM for hCA IX and 178–7950 nM for hCA XIV. Nevertheless, the inhibitor 6,7-dimethoxy-1-cyclopentyl-3,4-dihydroisoquinoline-2(1*H*)-sulfonamide (**9**) was ~ 3 -fold more active on hCA IX than hCA XIV (K_I of 55.0 nM versus K_I of 178.0 nM).

Interestingly some of these compounds showed higher selectivity for hCA IX and hCA XIV isoforms over the ubiquitous isoform hCA II, which can be considered an off-target. In fact, we found that for our newly synthesized CAIs **4–10** the selectivity ratios (see Table 1) for inhibiting hCA II over hCA IX were in the range 11.8–875, whereas their selectivity ratios for inhibiting hCA II over hCA XIV were in the range 128–778.

The most remarkable result is that the potent hCA IX and hCA XIV inhibitor 6,7-dimethoxy-1-isopropyl-3,4-dihydroisoquinoline-2(1*H*)-sulfonamide (**6**) is 172-fold and 223-fold more potent on hCA IX and hCA XIV than on hCA II. Moreover, the analysis of the selectivity ratio results highlighted that the presence of bulky C-1 substituents on isoquinoline scaffold led to the most selective inhibitors (e.g., **5** and **8**, with R_2 = propyl or butyl group) even if they are less potent than the compounds that bear small groups on tetrahydroisoquinoline skeleton (e.g., compounds **1–3**). Apparently for this class of compounds the introduction of cyclopropyl and isopropyl groups produces the optimization

of both potency and selectivity, suggesting that in this region there is a restrictive steric requirement for the catalytic binding site interaction. The enhancement of potency and selectivity was very significant when we compared the obtained results for compounds **1–10** with those of other known inhibitors such as acetazolamide, zonisamide, and topiramate (K_I values and selectivity ratios reported in Table 1).

Finally, by considering the results of the current assays with the biological data obtained for the earlier reported prototype (**I**) (see Table 1), it may be observed that the presence of a phenyl group at the C-1 position drives to a flat selectivity and poor inhibitory efficacy for all tested isoforms.²⁷ So the most important consideration is that the introduction of a suitable small (cyclo)alkyl group in proximity of sulfonamide function could influence its geometrical disposition in the catalytic binding site, thus controlling both the inhibitory potency and selectivity.

Crystallographic Studies. To determine the binding mode and decipher the key interactions contributing to the inhibitory properties for this class of 3,4-dihydroisoquinoline-2(1*H*)-sulfonamides, one of the most active compounds has been cocrystallized with hCA II. The statistics for data collection and refinement are summarized in Table 2. The crystal structure of hCA II in complex with 6,7-dimethoxy-3,4-dihydroisoquinoline-2(1*H*)-sulfonamide (**2**) was determined by difference Fourier techniques and refined using diffraction data to 1.65 Å resolution. The complex crystallized in the monoclinic $P2_1$ space group with one hCA II molecule in the asymmetric unit and solvent content of 41.3%. All hCA II residues could be traced into a well-defined electron density map with the exception of side chains of several terminal amino acid residues (Ser2, His3, His4, and Lys261) and side chains of two surface residues Lys9 and Lys133. During the course of the crystallographic refinement two continuous non-protein electron densities

Table 2. Crystal Data and Diffraction Data Collection and Refinement Statistics^a

| parameter | |
|-----------------------------------|---|
| data collection statistics | |
| space group | $P2_1$ |
| unit cell length (Å) | $a = 42.31, b = 41.27,$ $c = 72.04$ |
| angle (deg) | $\alpha = 90, \beta = 104.22,$ $\gamma = 90$ |
| no. of molecules in AU | 1 |
| wavelength (Å) | 1.5418 |
| resolution range (Å) | 19.95–1.65 (1.69–1.65) |
| no. of unique reflections | 26,928 |
| redundancy | 2.2 (2.2) |
| completeness (%) | 92.5 (88.6) |
| R_{merge}^b | 0.079 (0.362) |
| average $I/\sigma(I)$ | 5.9 (2.0) |
| Wilson B (Å ²) | 13.3 |
| refinement statistics | |
| resolution range (Å) | 19.95–1.65 (1.69–1.65) |
| no. of reflections in working set | 25556 (1811) |
| no. of reflections in test set | 1353 (84) |
| R^c (%) | 16.08 (22.40) |
| R_{free}^d (%) | 19.55 (28.90) |
| rmsd bond length (Å) | 0.011 |
| rmsd angle (deg) | 1.43 |
| no. of atoms in AU | 4949 |
| no. of protein atoms in AU | 4138 |
| no. of water molecules in AU | 237 |
| mean B (Å ²) | 14.0 |
| Ramachandran plot statistics | |
| residues in favored regions (%) | 97.3 |
| residues in allowed regions (%) | 2.7 |
| PDB code | 3IGP |

^aThe data in parentheses refer to the highest-resolution shell.

^b $R_{\text{merge}} = \sum_{hkl} \sum_i |I_i(hkl) - \langle I(hkl) \rangle| / \sum_{hkl} \sum_i I_i(hkl)$, where the $I_i(hkl)$ is an individual intensity of the i th observation of reflection hkl and $\langle I(hkl) \rangle$ is the average intensity of reflection hkl with summation over all data.

^c $R = \sum ||F_o| - |F_c|| / \sum |F_o|$, where F_o and F_c are the observed and calculated structure factors, respectively.

^d R_{free} is equivalent to R but is calculated for 5% of the reflections chosen at random and omitted from the refinement process.⁵⁸

were noticeable in the active site and on the surface of the molecule, respectively; both could be unambiguously modeled as the 6,7-dimethoxy-3,4-dihydroisoquinoline-2(1*H*)-sulfonamide (**2**).

As shown in Figure 1, the compound **2** binds into the cavity of the hCA II active site with the deeply buried sulfonamide group. The ionized nitrogen atom of the sulfonamide moiety is coordinated to the zinc ion at a distance of 2.07 Å. The sulfonamide nitrogen also donates a hydrogen bond to O γ of Thr199, and one oxygen from the sulfonamide moiety forms a hydrogen bond with backbone amine group of Thr199 (Figure 1). These key hydrogen bonds between the sulfonamide moiety of the inhibitor and enzyme active site are also found in other structurally characterized hCA II–sulfonamide complexes.^{4,11,29,30}

The sulfonamide moiety seems to serve as an anchor for specific binding of compound **2** into the enzyme active site. In addition to the polar interactions mediated by the sulfonamide group, hydrophobic interactions of the (substituted) isoquinoline moiety strongly stabilize the inhibitor within the active site cavity. The isoquinoline moiety forms numerous van der Waals interactions (distance of < 4.2 Å) with the bottom of the active site (residues Gln92, Val121, Val143, Trp209) and the loop formed by residues Ser197–Pro202.

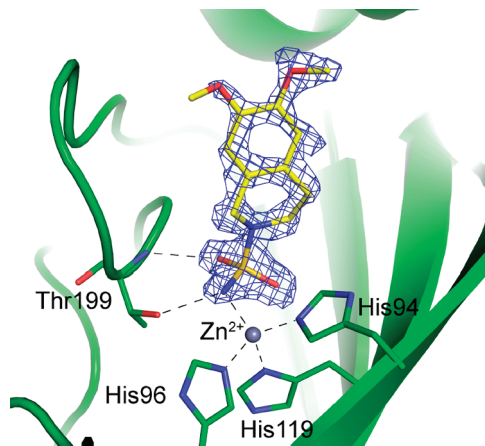


Figure 1. Binding of 6,7-dimethoxy-3,4-dihydroisoquinoline-2(1*H*)-sulfonamide (**2**) to the hCA II. Detail of the hCA II active site with the inhibitor represented as a stick model (with carbon and oxygen atoms colored yellow and red, respectively). The $2F_o - F_c$ electron density maps are contoured at 1.5σ . Protein is represented in green as a cartoon model with residues forming polar contacts with inhibitor highlighted in sticks. Also three histidine residues coordinating zinc ion are shown.

Also, the side chain of Phe131 from helix 4 contributes to interaction with the substituting methoxy-groups (Table S1 in Supporting Information). In the vicinity of the inhibitor, a glycerol molecule could be modeled into the hCA II active site, making hydrogen bonds with Asn62, Asn67, and Gln92 (Figure S1 in Supporting Information). The binding of glycerol to an identical site was also observed in several other hCA II–inhibitor complexes (e.g., 2NNG, 2NNS, 2NNO, 2NNV²⁹). Glycerol was used at high concentration (20% v/v) for crystal cryoprotection, and its binding probably represents a crystallization artifact.

Also, the inhibitor second binding site identified on the protein surface probably has no biological relevance and represents a crystallization artifact caused by high concentrations of inhibitor employed in the cocrystallization experiments. The inhibitor **2** interacts through direct hydrogen bonds with surface residues His15 and Asp19 and through a water mediated hydrogen bond with Ser2 (Figure S2 in Supporting Information). This inhibitor second binding site is also occupied by sulfonamide inhibitors in other hCA II–inhibitor complexes (e.g., PDB codes 2FOS, 2FOV, 2FOQ, 2FOU;³¹ 2NNO, 2NNS, 2NNV;²⁹ and 1ZFQ).

The inhibitor binding does not cause any major structural changes to the protein; the root-mean-square deviation (rmsd) for superposition of 256 C α atoms (residues 4–259) of our complex structure with free hCA II (PDB code 1CA2³⁰) is 0.34 Å, which is below the value observed for identical structures.³²

Docking Studies. With the aim to clarify the differences observed in the affinity and selectivity of our compounds toward hCA IX or hCA XIV over hCA II, preliminary docking analysis³³ has been also performed. These computational studies were carried out using crystal structures of hCA II, hCA IX, and hCA XIV complexed with acetazolamide from the RCSB Protein Data Bank (1YDB,³⁴ 3IAI,³⁵ and 1RJ6³⁶). Then we docked the most active compound 6, 7-dimethoxy-1-isopropyl-3,4-dihydroisoquinoline-2(1*H*)-sulfonamide (**6**) in the active site (see details in Experimental Section). The active sites of hCA II, hCA IX, and hCA XIV isoforms appear as a compact globular domain, located in a

large conical cavity that spans from the surface to the center of the protein, and present only minor differences in the region 125–137 and in the loop incorporating residues 198–204.³⁵ In particular, the hCA II residues Phe131, Val135, and Leu204 are replaced by Val131, Leu135, and Ala204 (hCA IX) and by Leu131, Ala135, and Tyr204 (hCA XIV).

Figure 2 displays the superposition of docking pose of compound **6** with X-ray position of acetazolamide in hCA II. Moreover, it also shows the X-ray position of **2** (see X-ray section) obtained through protein backbone-based structural superposition. It is possible to note that in all three inhibitors the sulfonamide groups assume similar orientations, sharing the key hydrogen bond interactions with the zinc ion and Thr199. The acetazolamide and compound **2**

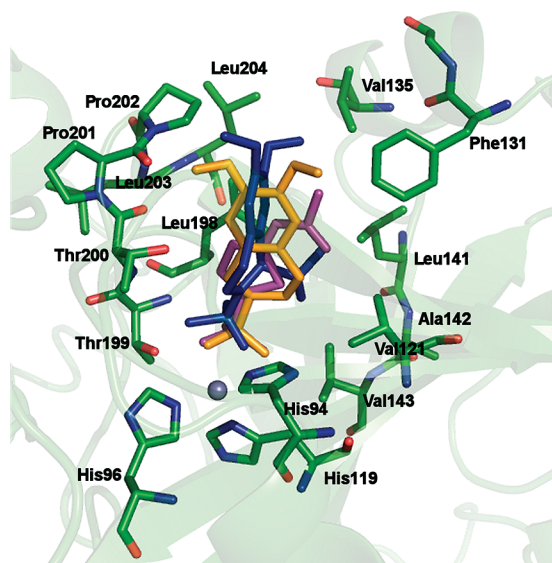


Figure 2. Superposition of inhibitors (acetazolamide, **2** and **6**) into the hCA II catalytic site. The residues participating in recognition of the inhibitors and the catalytic triad (His94, His96, and His119) coordinating zinc ion are also shown. The zinc ion is shown as a gray sphere. Acetazolamide is reported in magenta, **2** in orange, and **6** in blue.

show a very similar binding mode stabilized by both interactions with the loop and a hydrophobic contact with residue Phe131, whereas the compound **6** appears locked in a different orientation, probably due to hydrophobic interactions with Val121, Ala142, and Ala143, through the isopropyl moiety. In this disposition compound **6** lacks the interaction with the loop, thus explaining its lower hCA II inhibitory activity (Table 1). Figure 3 shows the docking results of compound **6** compared with the X-ray position of acetazolamide in complex with hCA IX (Figure 3A) and hCA XIV (Figure 3B). It is possible to observe (Figures 3) that the acetazolamide presents the same sort of interactions as well as similar K_i values (Table 1), whereas compound **6** seems able to establish new additional hydrophobic interactions with the residues Leu135/Ala204 (hCA IX) and Ala135/Tyr204 (hCA XIV), located in the upper part of the binding site, thus justifying the selectivity ratios reported in Table 1.

Conclusions

We have identified new isoquinoline derivatives containing sulfonamide moiety that showed very high affinity toward tumor-associated isoform hCA IX as well as neuronal hCA XIV displaying inhibitory effects at nanomolar concentration. In addition, these new compounds proved to be selective CAIs with significant selectivity ratios for inhibiting hCA IX over hCA II in the range 8.86–875 and for inhibiting hCA XIV over hCA II in the range 9.09–778. This study furnished some SAR consideration for this new class of CAIs, suggesting that the nature of the C-1 substituent on the isoquinoline scaffold could play a key role in the inhibitory effects. Considering the importance and the difficulty of obtaining selective CAIs, these results give relevant insights useful for designing new inhibitors having low affinity to the physiological ubiquitous hCA I and hCA II but maintaining inhibitory activity on other druggable isoforms. By X-ray crystallography, we confirmed that these inhibitors could bind the catalytic site of CAs through the sulfonamide moiety. In particular, we studied one of the most active 3,4-dihydroisoquinoline-2(1*H*)-sulfonamide derivative (**2**) in complex with hCA II. Moreover, the key interactions promoting the hCA IX and hCA XIV activity

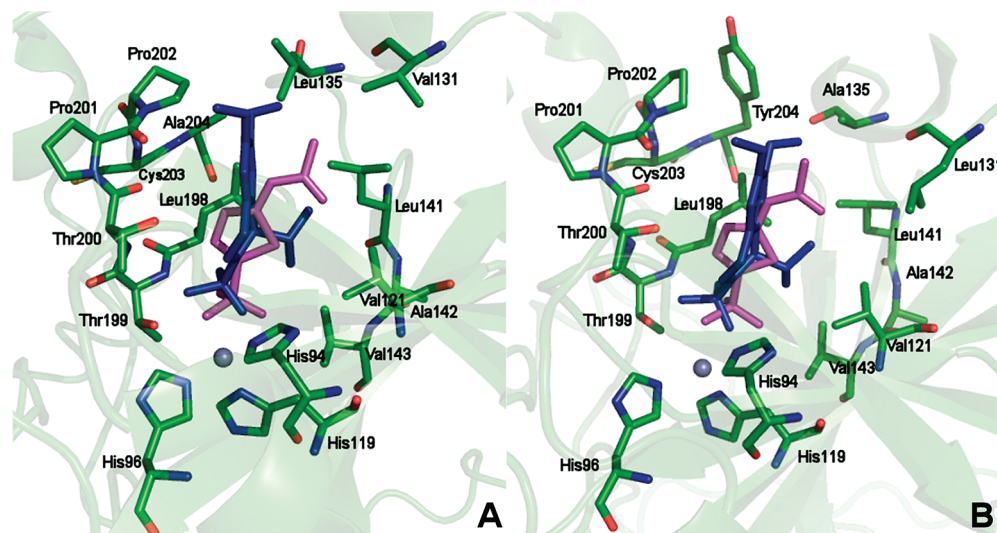


Figure 3. Structures of hCA IX (A) and hCA XIV (B) in complex with acetazolamide (magenta) overlaid with docked structure of compound **6** (blue). The residues participating in recognition of the inhibitors and the three histidine residues coordinating zinc ion are also shown. The zinc ion is shown as gray sphere.

and selectivity of compound **6** were analyzed by docking experiments.

Experimental Section

Chemistry. All reagents were purchased from Sigma Aldrich and were used without further purification. Microwave-assisted reactions were carried out in a CEM focused microwave synthesis system. Melting points were determined on a Buchi melting point B-545 apparatus and are uncorrected. Elemental analyses (C, H, N) were carried out on a Carlo Erba model 1106 elemental analyzer, and the results are within $\pm 0.4\%$ of the theoretical values. Merck silica gel 60 F254 plates were used for analytical TLC; R_f values were determined employing TLC plates and using $\text{CHCl}_3/\text{MeOH}$ (95:5) as eluent. ^1H NMR and ^{13}C NMR spectra were measured in CDCl_3 (TMS as internal standard) or $\text{DMSO}-d_6$ with a Varian Gemini 300 spectrometer; chemical shifts are expressed in δ (ppm) and coupling constants (J) in Hz. All exchangeable protons were confirmed by addition of deuterium oxide (D_2O). GC-MS spectra for selected compounds were recorded on a Shimadzu QP500 EI 151 mass spectrometer (see Supporting Information).

General Procedure for the Synthesis of 1-(Cyclo)alkyl-6,7-dimethoxy-1,2,3,4-tetrahydroisoquinolines (22–29). The new one-pot procedure for the synthesis of free amines **22–29** was carried out in microwave assisted conditions starting from commercially available 2-(3',4'-dimethoxyphenyl)ethylamine (**13**) and the suitable aldehydes via imine intermediates **14–21** following a previously reported synthetic approach to obtain 1-aryl-6,7-dimethoxy-1,2,3,4-tetrahydroisoquinolines.^{27,28} Analytical and spectroscopic data for the isoquinoline derivatives **22–29** are in accordance with literature results.^{37–40}

General Procedure for the Synthesis of 3,4-Dihydroisoquinoline-2(1H)-sulfonamides (1–10). A mixture of the appropriate 1,2,3,4-tetrahydroisoquinoline (**11**) or 6,7-dimethoxy-1,2,3,4-tetrahydroisoquinoline (**12**, **22–29**) (1.0 mmol) and sulfamide (6 mmol, 576 mg) in dimethoxyethane (2 mL) was placed in a cylindrical quartz tube ($\varnothing 2$ cm), then stirred and irradiated in a microwave oven at 150 W for two steps of 20 min at 90 °C. The reaction was quenched by adding water (5 mL) and extracted with ethyl acetate (3×5 mL). The organic layer was washed with an aqueous saturated solution of NaHCO_3 (2×5 mL), dried over Na_2SO_4 , and concentrated until dryness under reduced pressure. The residue crystallized from diethyl ether to give the desired compounds **1–10**.

3,4-Dihydroisoquinoline-2(1H)-sulfonamide (1). Yield 43%; mp 161–163 °C. $R_f = 0.415$. ^1H NMR ($\text{DMSO}-d_6$) δ 2.89 (t, $J = 5.77$, 2H, CH_2), 3.24 (t, $J = 5.77$, 2H, CH_2), 4.18 (s, 2H, CH_2), 6.91 (bs, 2H, NH_2), 7.15 (s, 4H, ArH). Anal. ($\text{C}_9\text{H}_{12}\text{N}_2\text{O}_2\text{S}$) C, H, N.

6,7-Dimethoxy-3,4-dihydroisoquinoline-2(1H)-sulfonamide (2). Yield 51%; mp 164–166 °C. $R_f = 0.405$. ^1H NMR ($\text{DMSO}-d_6$) δ 2.79–2.81 (m, 2H, CH_2), 3.19–3.23 (m, 2H, CH_2), 3.70 (s, 6H, OCH_3), 4.09 (s, 2H, CH_2), 6.71 (s, 1H, ArH), 6.72 (s, 1H, ArH), 6.85 (bs, 2H, NH_2). Anal. ($\text{C}_{11}\text{H}_{16}\text{N}_2\text{O}_4\text{S}$) C, H, N.

6,7-Dimethoxy-1-methyl-3,4-dihydroisoquinoline-2(1H)-sulfonamide (3). Yield 35%; mp 172–174 °C. $R_f = 0.465$. ^1H NMR (CDCl_3) δ 1.54 (d, $J = 6.87$, 3H, CH_3), 2.64–2.70 (m, 1H, CH), 2.96–3.12 (m, 1H, CH), 3.35–3.45 (m, 1H, CH), 3.82–3.95 (m, 1H, CH), 3.85 (s, 3H, OCH_3), 3.86 (s, 3H, OCH_3), 4.35 (bs, 2H, NH_2), 4.95 (q, $J = 6.87$, 1H, CH), 6.56 (s, 1H, ArH), 6.59 (s, 1H, ArH). Anal. ($\text{C}_{12}\text{H}_{18}\text{N}_2\text{O}_4\text{S}$) C, H, N.

6,7-Dimethoxy-1-ethyl-3,4-dihydroisoquinoline-2(1H)-sulfonamide (4). Yield 33%; mp 201–203 °C. $R_f = 0.470$. ^1H NMR (CDCl_3) δ 1.07 (t, $J = 7.42$, 3H, CH_3), 1.75–1.85 (m, 2H, CH_2), 2.60–2.66 (m, 1H, CH), 3.04–3.16 (m, 1H, CH), 3.36–3.47 (m, 1H, CH), 3.78–3.99 (m, 1H, CH), 3.85 (s, 3H, OCH_3), 3.86 (s, 3H, OCH_3), 4.27 (bs, 2H, NH_2), 4.61–4.66 (m, 1H, CH), 6.57 (s, 1H, ArH), 6.59 (s, 1H, ArH). Anal. ($\text{C}_{13}\text{H}_{20}\text{N}_2\text{O}_4\text{S}$) C, H, N.

6,7-Dimethoxy-1-propyl-3,4-dihydroisoquinoline-2(1H)-sulfonamide (5). Yield 46%. Mp 185–187 °C. $R_f = 0.520$. ^1H NMR (CDCl_3) δ 0.98 (t, $J = 7.42$, 3H, CH_3), 1.48–1.81 (m, 4H, $\text{CH}_2\text{--CH}_2$), 2.60–2.66 (m, 1H, CH), 3.04–3.16 (m, 1H, CH), 3.38–3.48 (m, 1H, CH), 3.85 (s, 3H, OCH_3), 3.87 (s, 3H, OCH_3), 3.93–4.00 (m, 1H, CH), 4.27 (bs, 2H, NH_2), 4.70–4.74 (m, 1H, CH), 6.56 (s, 1H, ArH), 6.58 (s, 1H, ArH). Anal. ($\text{C}_{14}\text{H}_{22}\text{N}_2\text{O}_4\text{S}$) C, H, N.

6,7-Dimethoxy-1-isopropyl-3,4-dihydroisoquinoline-2(1H)-sulfonamide (6). Yield 44%; mp 187–189 °C. $R_f = 0.505$. ^1H NMR ($\text{DMSO}-d_6$) δ 0.86–0.90 (m, 6H, CH_3), 1.96–2.02 (m, 1H, CH), 2.57–2.62 (m, 1H, CH), 2.84–2.92 (m, 1H, CH), 3.33–3.39 (m, 1H, CH), 3.48–3.56 (m, 1H, CH), 3.70 (s, 6H, OCH_3), 4.27 (d, $J = 7.14$, 1H, CH), 6.57 (bs, 2H, NH_2), 6.68 (s, 1H, ArH), 6.70 (s, 1H, ArH). Anal. ($\text{C}_{14}\text{H}_{22}\text{N}_2\text{O}_4\text{S}$) C, H, N.

1-Cyclopropyl-6,7-dimethoxy-3,4-dihydroisoquinoline-2(1H)-sulfonamide (7). Yield 35%; mp 217–219 °C. $R_f = 0.468$. ^1H NMR ($\text{DMSO}-d_6$) δ 0.42–0.61 (m, 4H, CH_2), 1.13–1.17 (m, 1H, CH), 2.55–2.60 (m, 1H, CH), 2.88–2.99 (m, 1H, CH), 3.34–3.65 (m, 2H, CH), 3.99 (d, $J = 7.14$, 1H), 6.62 (bs, 2H, NH_2), 6.68 (s, 1H, ArH), 6.76 (s, 1H, ArH). Anal. ($\text{C}_{14}\text{H}_{20}\text{N}_2\text{O}_4\text{S}$) C, H, N.

1-*n*-Butyl-6,7-dimethoxy-3,4-dihydroisoquinoline-2(1H)-sulfonamide (8). Yield 60%; mp 171–173 °C. $R_f = 0.533$. ^1H NMR (CDCl_3) δ 0.93 (t, $J = 7.42$, 3H, CH_3), 1.25–1.81 (m, 6H, $\text{CH}_2\text{--CH}_2\text{--CH}_2$), 2.60–2.66 (m, 1H, CH), 3.07–3.16 (m, 1H, CH), 3.38–3.48 (m, 1H, CH), 3.85 (s, 3H, OCH_3), 3.86 (s, 3H, OCH_3), 3.93–4.00 (m, 1H, CH), 4.28 (bs, 2H, NH_2), 4.68–4.73 (m, 1H, CH), 6.56 (s, 1H, ArH), 6.58 (s, 1H, ArH). Anal. ($\text{C}_{15}\text{H}_{24}\text{N}_2\text{O}_4\text{S}$) C, H, N.

1-Cyclopentyl-6,7-dimethoxy-3,4-dihydroisoquinoline-2(1H)-sulfonamide (9). Yield 67%; mp 193–195 °C. $R_f = 0.575$. ^1H NMR (CDCl_3) δ 1.39–1.92 (m, 9H, CH), 2.13–2.16 (m, 1H, CH), 2.71–2.76 (m, 1H, CH), 3.07–3.09 (m, 1H, CH), 3.53–3.61 (m, 1H, CH), 3.86 (s, 6H, OCH_3), 3.91–3.98 (m, 1H, CH), 4.17 (bs, 2H, NH_2), 4.45 (d, $J = 8.89$, 1H), 6.60 (s, 1H, ArH), 6.63 (s, 1H, ArH). Anal. ($\text{C}_{16}\text{H}_{24}\text{N}_2\text{O}_4\text{S}$) C, H, N.

1-Cyclohexyl-6,7-dimethoxy-3,4-dihydroisoquinoline-2(1H)-sulfonamide (10). Yield 34%; mp 177–179 °C. $R_f = 0.560$. ^1H NMR (CDCl_3) δ 1.03–1.99 (m, 11H, CH), 2.73–2.80 (m, 1H, CH), 2.98–3.11 (m, 1H, CH), 3.48–3.61 (m, 1H, CH), 3.83–3.90 (m, 1H, CH), 3.85 (s, 3H, OCH_3), 3.86 (s, 3H, OCH_3), 4.09 (bs, 2H, NH_2), 4.37 (d, $J = 8.79$, 1H, CH), 6.57 (s, 1H, ArH), 6.62 (s, 1H, ArH). Anal. ($\text{C}_{17}\text{H}_{26}\text{N}_2\text{O}_4\text{S}$) C, H, N.

CA Inhibition Assay. An Applied Photophysics stopped-flow instrument has been used for assaying the CA catalyzed CO_2 hydration activity.⁴¹ Phenol red (at a concentration of 0.2 mM) has been used as indicator, working at the absorbance maximum of 557 nm, with 10–20 mM Hepes (pH 7.5) or Tris (pH 8.3) as buffers and 20 mM Na_2SO_4 or 20 mM NaClO_4 (for maintaining constant the ionic strength), following the initial rates of the CA-catalyzed CO_2 hydration reaction for a period of 10–100 s. The CO_2 concentrations ranged from 1.7 to 17 mM for the determination of the kinetic parameters and inhibition constants. For each inhibitor at least six traces of the initial 5–10% of the reaction have been used for determining the initial velocity. The uncatalyzed rates were determined in the same manner and subtracted from the total observed rates. Stock solutions of inhibitor (10 mM) were prepared in distilled–deionized water, and dilutions up to 0.01 nM were done thereafter with distilled–deionized water. Inhibitor and enzyme solutions were preincubated together for 15 min at room temperature prior to assay in order to allow for the formation of the E–I complex. The inhibition constants were obtained by nonlinear least-squares methods using PRISM 3, as reported earlier, and represent the mean from at least three different determinations. CA isoforms were recombinant ones obtained as reported earlier by this group.^{42–45}

Protein Crystallography. Protein Crystallization and X-ray Data Collection. The complex was prepared by adding 5-fold

molar excess of 6,7-dimethoxy-3,4-dihydroisoquinoline-2(1*H*)-sulfonamide (**2**) (in dimethyl sulfoxide) to 10 mg·mL⁻¹ protein solution of hCA II (Sigma) in 100 mM Tris-Cl, pH 8.5. The best crystals of the complex were obtained by the hanging-drop vapor diffusion method, under the following conditions: an amount of 2 μ L of complex solution was mixed with 2 μ L of precipitant solution [2.5 M (NH₄)₂SO₄, 0.3 M NaCl, 100 mM Tris-Cl, pH 8.2] and equilibrated over a reservoir containing 1 mL of precipitant solution at 18 °C. Crystals with dimensions 0.4 mm \times 0.2 mm \times 0.1 mm grew within 10 days.

For data collection, the crystals were soaked in the reservoir solution supplemented with 20% (v/v) glycerol and transferred to liquid nitrogen. Diffraction data were collected at 120 K using an in-house diffractometer (Nonius FR 591) connected to 345 mm MarResearch image plate detector. The best crystal diffracted up to 1.65 Å resolution, and diffraction data were integrated and reduced using MOSFLM⁴⁶ and scaled using SCALA⁴⁷ from the CCP4 suite of programs.⁴⁸ Crystal parameters and data collection statistics are summarized in Table 2.

Structure Determination, Refinement, and Analysis. The structure of hCA II in complex with 6,7-dimethoxy-3,4-dihydroisoquinoline-2(1*H*)-sulfonamide (**2**) was solved using the difference Fourier method, using hCA II structure (Protein Data Bank entry 1H9N⁴⁹) as the initial model. Initial rigid-body refinement and subsequent restrained refinement were performed using the program REFMAC 5.⁴⁸ The structure was refined with two inhibitor molecules, one in the enzyme active site and the other located in the surface pocket in the vicinity of the enzyme N-terminus. Atomic coordinates and geometry library for the inhibitor were generated using the PRODRG server.⁵⁰ The Coot program⁵¹ was used for inhibitor fitting, model rebuilding, and addition of water molecules. In final refinement stages, TLS refinement cycles in the program REFMAC 5 were introduced.⁵² The quality of the crystallographic model was assessed with MolProbity.⁵³ Program CONTACT/ACT from the CCP4 suite⁴⁸ was used for finding contacts between inhibitor and protein molecules. The final refinement statistics are summarized in Table 2. All figures showing structural representations were prepared using PyMOL,⁵⁴ and the APBS⁵⁵ tools plugin was used for generating solvent accessible surface colored by electrostatic potential.

Docking Studies. The crystal structures of hCA II, hCA IX, and hCA XIV in complex with the inhibitor acetazolamide were retrieved from the RCSB Protein Data Bank (entry code 1YDB,³⁴ 3IAI,³⁵ and 1RJ6³⁶). The complex 1YDB presents the mutant Phe198; thus, for our docking studies, it was converted in Leu198, placing its side chain in the same position observed in our X-ray crystal structure of hCAII. Hydrogen atoms were added to proteins by the Biopolymer module in SYBYL 8.0.1.⁵⁶ The acetazolamide structure was extracted from an X-ray complex, and the other structures of the ligands were constructed using standard bond lengths and angles from the SYBYL 8.0 fragment library. All inhibitors were fully optimized by the semiempirical quantum mechanical method AM1. The ligands minimized in this way were docked in their corresponding proteins by means of Gold 3.1.1.³³ The region of interest used by Gold was defined in order to contain the residues within 10 Å from the original position of the ligand in the X-ray structures; the zinc ion was set as possessing a trigonal-bipyramidal coordination. The "allow early termination" command was deactivated, while the possibility for the ligand to flip ring corners was activated. ChemScore³³ was chosen as the fitness function, and the formation of a H bond between the hydroxyl group of Thr199 and the ligands was also imposed.⁵⁷ As regards to all the other parameters, the Gold default ones were used, and the ligands were submitted to 100 genetic algorithm runs.

Acknowledgment. Financial support for this research by Fondo di Ateneo per la Ricerca (PRA 2006, Università di

Messina) is gratefully acknowledged. Research from CTS lab was financed by a grant of the sixth Framework Programme (FP) of the European Union (Project DeZnIT) and by a seventh FP grant (Project METOXIA). In part, this work was supported by Projects AV0Z50520514 and AV0Z40550506 awarded by the Academy of Sciences of the Czech Republic, grant No. 1M0505 awarded by the Ministry of Education of the Czech Republic, and grant No. GA203/09/0820 awarded by Czech Grant Foundation. P. Mader is a PhD student registered at the First Faculty of Medicine, Charles University in Prague.

Supporting Information Available: Other spectroscopic and crystal data; table of contacts between inhibitor and protein. This material is available free of charge via the Internet at <http://pubs.acs.org>.

References

- (1) Thiry, A.; Dogne, J. M.; Supuran, C. T.; Masereel, B. Carbonic anhydrase inhibitors as anticonvulsant agents. *Curr. Top. Med. Chem.* **2007**, *7*, 855–864.
- (2) Supuran, C. T.; Di Fiore, A.; De Simone, G. Carbonic anhydrase inhibitors as emerging drugs for the treatment of obesity. *Expert Opin. Emerging Drugs* **2008**, *13*, 383–392.
- (3) Pastorekova, S.; Kopacek, J.; Pastorek, J. Carbonic anhydrase inhibitors and the management of cancer. *Curr. Top. Med. Chem.* **2007**, *7*, 865–878.
- (4) Supuran, C. T.; Scozzafava, A.; Casini, A. Carbonic anhydrase inhibitors. *Med. Res. Rev.* **2003**, *23*, 146–189.
- (5) Supuran, C. T. Carbonic anhydrases: novel therapeutic applications for inhibitors and activators. *Nat. Rev. Drug Discovery* **2008**, *7*, 168–181.
- (6) Winum, J. Y.; Poulsen, S. A.; Supuran, C. T. Therapeutic applications of glycosidic carbonic anhydrase inhibitors. *Med. Res. Rev.* **2009**, *29*, 419–435.
- (7) Guzel, O.; Temperini, C.; Innocenti, A.; Scozzafava, A.; Salman, A.; Supuran, C. T. Carbonic anhydrase inhibitors. Interaction of 2-(hydrazinocarbonyl)-3-phenyl-1*H*-indole-5-sulfonamide with 12 mammalian isoforms: kinetic and X-ray crystallographic studies. *Bioorg. Med. Chem. Lett.* **2008**, *18*, 152–158.
- (8) Thiry, A.; Supuran, C. T.; Masereel, B.; Dogne, J. M. Recent developments of carbonic anhydrase inhibitors as potential anticancer drugs. *J. Med. Chem.* **2008**, *51*, 3051–3056.
- (9) Chiche, J.; Ilc, K.; Laferriere, J.; Trotter, E.; Dayan, F.; Mazure, N. M.; Brahimi-Horn, M. C.; Pouyssegur, J. Hypoxia-inducible carbonic anhydrase IX and XII promote tumor cell growth by counteracting acidosis through the regulation of the intracellular pH. *Cancer Res.* **2009**, *69*, 358–368.
- (10) Parkkila, S.; Parkkila, A. K.; Rajaniemi, H.; Shah, G. N.; Grubb, J. H.; Waheed, A.; Sly, W. S. Expression of membrane-associated carbonic anhydrase XIV on neurons and axons in mouse and human brain. *Proc. Natl. Acad. Sci. U.S.A.* **2001**, *98*, 1918–1923.
- (11) Winum, J. Y.; Scozzafava, A.; Montero, J. L.; Supuran, C. T. Sulfamates and their therapeutic potential. *Med. Res. Rev.* **2005**, *25*, 186–228.
- (12) Winum, J. Y.; Scozzafava, A.; Montero, J. L.; Supuran, C. T. Therapeutic potential of sulfamides as enzyme inhibitors. *Med. Res. Rev.* **2006**, *26*, 767–792.
- (13) Supuran, C. T.; Casini, A.; Scozzafava, A. Protease inhibitors of the sulfonamide type: anticancer, antiinflammatory, and antiviral agents. *Med. Res. Rev.* **2003**, *23*, 535–558.
- (14) Winum, J. Y.; Scozzafava, A.; Montero, J. L.; Supuran, C. T. New zinc binding motifs in the design of selective carbonic anhydrase inhibitors. *Mini-Rev. Med. Chem.* **2006**, *6*, 921–936.
- (15) Supuran, C. T. Diuretics: from classical carbonic anhydrase inhibitors to novel applications of the sulfonamides. *Curr. Pharm. Des.* **2008**, *14*, 641–648.
- (16) Nasr, G.; Petit, E.; Vullo, D.; Winum, J. Y.; Supuran, C. T.; Barboiu, M. Carbonic anhydrase-encoded dynamic constitutional libraries: toward the discovery of isozyme-specific inhibitors. *J. Med. Chem.* **2009**, *52*, 853–859.
- (17) D'Ambrosio, K.; Masereel, B.; Thiry, A.; Scozzafava, A.; Supuran, C. T.; De Simone, G. Carbonic anhydrase inhibitors: binding of indanesulfonamides to the human isoform II. *ChemMedChem* **2008**, *3*, 473–477.
- (18) Winum, J. Y.; Scozzafava, A.; Montero, J. L.; Supuran, C. T. Metal binding functions in the design of carbonic anhydrase inhibitors. *Curr. Top. Med. Chem.* **2007**, *7*, 835–848.

- (19) Temperini, C.; Cecchi, A.; Scozzafava, A.; Supuran, C. T. Carbonic anhydrase inhibitors. Comparison of chlorthalidone and indapamide X-ray crystal structures in adducts with isozyme II: when three water molecules and the keto-enol tautomerism make the difference. *J. Med. Chem.* **2009**, *52*, 322–328.
- (20) Abbate, F.; Casini, A.; Scozzafava, A.; Supuran, C. T. Carbonic anhydrase inhibitors: X-ray crystallographic structure of the adduct of human isozyme II with a topically acting antiglaucoma sulfonamide. *Bioorg. Med. Chem. Lett.* **2004**, *14*, 2357–2361.
- (21) Casini, A.; Antel, J.; Abbate, F.; Scozzafava, A.; David, S.; Waldeck, H.; Schafer, S.; Supuran, C. T. Carbonic anhydrase inhibitors: SAR and X-ray crystallographic study for the interaction of sugar sulfamates/sulfamides with isozymes I, II and IV. *Bioorg. Med. Chem. Lett.* **2003**, *13*, 841–845.
- (22) Di Fiore, A.; Monti, S. M.; Hilvo, M.; Parkkila, S.; Romano, V.; Scaloni, A.; Pedone, C.; Scozzafava, A.; Supuran, C. T.; De Simone, G. Crystal structure of human carbonic anhydrase XIII and its complex with the inhibitor acetazolamide. *Proteins* **2009**, *74*, 164–175.
- (23) Temperini, C.; Cecchi, A.; Scozzafava, A.; Supuran, C. T. Carbonic anhydrase inhibitors. Interaction of indapamide and related diuretics with 12 mammalian isozymes and X-ray crystallographic studies for the indapamide–isozyme II adduct. *Bioorg. Med. Chem. Lett.* **2008**, *18*, 2567–2573.
- (24) Winum, J. Y.; Temperini, C.; El Cheikh, K.; Innocenti, A.; Vullo, D.; Ciattini, S.; Montero, J. L.; Scozzafava, A.; Supuran, C. T. Carbonic anhydrase inhibitors: clash with Ala65 as a means for designing inhibitors with low affinity for the ubiquitous isozyme II, exemplified by the crystal structure of the topiramate sulfamide analogue. *J. Med. Chem.* **2006**, *49*, 7024–7031.
- (25) Alterio, V.; Vitale, R. M.; Monti, S. M.; Pedone, C.; Scozzafava, A.; Cecchi, A.; De Simone, G.; Supuran, C. T. Carbonic anhydrase inhibitors: X-ray and molecular modeling study for the interaction of a fluorescent antitumor sulfonamide with isozyme II and IX. *J. Am. Chem. Soc.* **2006**, *128*, 8329–8335.
- (26) Menchise, V.; De Simone, G.; Alterio, V.; Di Fiore, A.; Pedone, C.; Scozzafava, A.; Supuran, C. T. Carbonic anhydrase inhibitors: stacking with Phe131 determines active site binding region of inhibitors as exemplified by the X-ray crystal structure of a membrane-impermeant antitumor sulfonamide complexed with isozyme II. *J. Med. Chem.* **2005**, *48*, 5721–5727.
- (27) Gitto, R.; Ferro, S.; Agnello, S.; De Luca, L.; De Sarro, G.; Russo, E.; Vullo, D.; Supuran, C. T.; Chimirri, A. Synthesis and evaluation of pharmacological profile of 1-aryl-6,7-dimethoxy-3,4-dihydroisoquinoline-2(1H)-sulfonamides. *Bioorg. Med. Chem.* **2009**, *17*, 3659–3664.
- (28) Gitto, R.; Ficarra, R.; Stancanelli, R.; Guardo, M.; De Luca, L.; Barreca, M. L.; Pagano, B.; Rotondo, A.; Bruno, G.; Russo, E.; De Sarro, G.; Chimirri, A. Synthesis, resolution, stereochemistry, and molecular modeling of (R)- and (S)-2-acetyl-1-(4'-chlorophenyl)-6,7-dimethoxy-1,2,3,4-tetrahydroisoquinoline AMPAR antagonists. *Bioorg. Med. Chem.* **2007**, *15*, 5417–5423.
- (29) Srivastava, D. K.; Jude, K. M.; Banerjee, A. L.; Haldar, M.; Manokaran, S.; Kooren, J.; Mallik, S.; Christianson, D. W. Structural analysis of charge discrimination in the binding of inhibitors to human carbonic anhydrases I and II. *J. Am. Chem. Soc.* **2007**, *129*, 5528–5537.
- (30) Eriksson, A. E.; Jones, T. A.; Liljas, A. Refined structure of human carbonic anhydrase II at 2.0 Å resolution. *Proteins* **1988**, *4*, 274–282.
- (31) Jude, K. M.; Banerjee, A. L.; Haldar, M. K.; Manokaran, S.; Roy, B.; Mallik, S.; Srivastava, D. K.; Christianson, D. W. Ultrahigh resolution crystal structures of human carbonic anhydrases I and II complexed with “two-prong” inhibitors reveal the molecular basis of high affinity. *J. Am. Chem. Soc.* **2006**, *128*, 3011–3018.
- (32) Betts, M. J.; Sternberg, M. J. An analysis of conformational changes on protein–protein association: implications for predictive docking. *Protein Eng.* **1999**, *12*, 271–283.
- (33) Jones, G.; Willett, P.; Glen, R. C.; Leach, A. R.; Taylor, R. Development and validation of a genetic algorithm for flexible docking. *J. Mol. Biol.* **1997**, *267*, 727–748.
- (34) Nair, S. K.; Krebs, J. F.; Christianson, D. W.; Fierke, C. A. Structural basis of inhibitor affinity to variants of human carbonic anhydrase II. *Biochemistry* **1995**, *34*, 3981–3989.
- (35) Alterio, V.; Hilvo, M.; Di Fiore, A.; Supuran, C. T.; Pan, P.; Parkkila, S.; Scaloni, A.; Pastorek, J.; Pastorekova, S.; Pedone, C.; Scozzafava, A.; Monti, S. M.; De Simone, G. Crystal structure of the catalytic domain of the tumor-associated human carbonic anhydrase IX. *Proc. Natl. Acad. Sci. U.S.A.* **2009**, *106*, 16233–16238.
- (36) Whittington, D. A.; Grubb, J. H.; Waheed, A.; Shah, G. N.; Sly, W. S.; Christianson, D. W. Expression, assay, and structure of the extracellular domain of murine carbonic anhydrase XIV: implications for selective inhibition of membrane-associated isozymes. *J. Biol. Chem.* **2004**, *279*, 7223–7228.
- (37) Craig, P. N.; Nabenhauer, F. P.; Williams, P. M.; Macko, E.; Toner, J. Tetrahydroisoquinolines. I. 1-Alkyl-6,7-dihydroxy-1,2,3,4-tetrahydroisoquinolines. *J. Am. Chem. Soc.* **1952**, *74*, 1316–1317.
- (38) Barbier, A. M.; Rumpf, P. Compounds related to emetine. I. Synthesis of 1-(1,2,3,4-tetrahydro-6,7-dimethoxy-1-propyl-2-isoquinolyl)-4-(1,2,3,4-tetrahydro-6,7-dimethoxy-1-isoquinolyl)butane acid oxalate. *Bull. Soc. Chim. Fr.* **1953**, 293–296.
- (39) Leseche, B.; Gilbert, J.; Viel, C. Study of the oxidation of 6,7- and 7,8-dimethoxytetrahydroisoquinolin-4-ols and the reactivity of the carbonyl group of 6,7-dimethoxytetrahydroisoquinol-4-one. *J. Heterocycl. Chem.* **1981**, *18*, 143–153.
- (40) Hegedues, A.; Hell, Z. One-step preparation of 1-substituted tetrahydroisoquinolines via the Pictet–Spengler reaction using zeolite catalysts. *Tetrahedron Lett.* **2004**, *45*, 8553–8555.
- (41) Khalifah, R. G. The carbon dioxide hydration activity of carbonic anhydrase. I. Stop-flow kinetic studies on the native human isoenzymes B and C. *J. Biol. Chem.* **1971**, *246*, 2561–2573.
- (42) Nishimori, I.; Vullo, D.; Innocenti, A.; Scozzafava, A.; Mastrolorenzo, A.; Supuran, C. T. Carbonic anhydrase inhibitors. The mitochondrial isozyme VB as a new target for sulfonamide and sulfamate inhibitors. *J. Med. Chem.* **2005**, *48*, 7860–7866.
- (43) Nishimori, I.; Vullo, D.; Innocenti, A.; Scozzafava, A.; Mastrolorenzo, A.; Supuran, C. T. Carbonic anhydrase inhibitors: inhibition of the transmembrane isozyme XIV with sulfonamides. *Bioorg. Med. Chem. Lett.* **2005**, *15*, 3828–3833.
- (44) Nishimori, I.; Minakuchi, T.; Onishi, S.; Vullo, D.; Scozzafava, A.; Supuran, C. T. Carbonic anhydrase inhibitors. DNA cloning, characterization, and inhibition studies of the human secretory isoform VI, a new target for sulfonamide and sulfamate inhibitors. *J. Med. Chem.* **2007**, *50*, 381–388.
- (45) Nishimori, I.; Minakuchi, T.; Morimoto, K.; Sano, S.; Onishi, S.; Takeuchi, H.; Vullo, D.; Scozzafava, A.; Supuran, C. T. Carbonic anhydrase inhibitors: DNA cloning and inhibition studies of the alpha-carbonic anhydrase from *Helicobacter pylori*, a new target for developing sulfonamide and sulfamate gastric drugs. *J. Med. Chem.* **2006**, *49*, 2117–2126.
- (46) Leslie, A. G. W. Integration of macromolecular diffraction data. *Acta Crystallogr., Sect. D: Biol. Crystallogr.* **1999**, *55*, 1696–1702.
- (47) Evans, P. R. In *Proceedings of the CCP4 Study Weekend. Data Collection and Processing*; Daresbury Laboratory: Warrington, U.K., 1993.
- (48) The CCP4 suite: programs for protein crystallography. *Acta Crystallogr., Sect. D: Biol. Crystallogr.* **1994**, *50*, 760–763.
- (49) Lesburg, C. A.; Huang, C.; Christianson, D. W.; Fierke, C. A. Histidine → carboxamide ligand substitutions in the zinc binding site of carbonic anhydrase II alter metal coordination geometry but retain catalytic activity. *Biochemistry* **1997**, *36*, 15780–15791.
- (50) Schuttelkopf, A. W.; van Aalten, D. M. PRODRG: a tool for high-throughput crystallography of protein–ligand complexes. *Acta Crystallogr., Sect. D: Biol. Crystallogr.* **2004**, *60*, 1355–1363.
- (51) Emsley, P.; Cowtan, K. Coot: model-building tools for molecular graphics. *Acta Crystallogr., Sect. D: Biol. Crystallogr.* **2004**, *60*, 2126–2132.
- (52) Winn, M. D.; Isupov, M. N.; Murshudov, G. N. Use of TLS parameters to model anisotropic displacements in macromolecular refinement. *Acta Crystallogr., Sect. D: Biol. Crystallogr.* **2001**, *57*, 122–133.
- (53) Lovell, S. C.; Davis, I. W.; Arendall, W. B., 3rd; de Bakker, P. I.; Word, J. M.; Prisant, M. G.; Richardson, J. S.; Richardson, D. C. Structure validation by Cα geometry: phi, psi and Cβ deviation. *Proteins* **2003**, *50*, 437–450.
- (54) De Lano, W. L. *The PyMOL Molecular Graphics System*; DeLano Scientific: Palo Alto, CA, 2002.
- (55) Baker, N. A.; Sept, D.; Joseph, S.; Holst, M. J.; McCammon, J. A. Electrostatics of nanosystems: application to microtubules and the ribosome. *Proc. Natl. Acad. Sci. U.S.A.* **2001**, *98*, 10037–10041.
- (56) SYBYL, version 8.0; Tripos Inc. (1699 South Hanley Road, St. Louis, MO 63144), 2005.
- (57) Tuccinardi, T.; Nuti, E.; Ortore, G.; Supuran, C. T.; Rossello, A.; Martinelli, A. Analysis of human carbonic anhydrase II: docking reliability and receptor-based 3D-QSAR study. *J. Chem. Inf. Model.* **2007**, *47*, 515–525.
- (58) Brunger, A. T. Free R value: a novel statistical quantity for assessing the accuracy of crystal structures. *Nature* **1992**, *355*, 472–475.